Journal of Cerebral Blood Flow & Metabolism (2014) 34, 1599–1603

www.jcbfm.com

BRIEF COMMUNICATION

Functional MRI in mice lacking IP_3-dependent calcium signaling in astrocytes

Pierrick Jego[1], Jesús Pacheco-Torres[1], Alfonso Araque[2,3] and Santiago Canals[1]

Functional magnetic resonance imaging (fMRI) is a fundamental tool to investigate human brain networks. However, the cellular mechanisms underlying fMRI signals are not fully understood. One hypothetical mechanism is the putative vascular control exerted by cytosolic calcium in perivascular astrocytes. We have performed combined fMRI-electrophysiology experiments in mice lacking the inositol 1,4,5-triphosphate-type-2 receptor, with the primary pathway of cytosolic calcium increase eliminated into astrocytes. Our results show that evoked electrophysiologic activity and fMRI signals acquired during either transient or sustained neuronal activations occur independently of these large calcium signals. This result challenges the suggested intermediary role of astrocytic calcium surges in fMRI-signal generation.

Journal of Cerebral Blood Flow & Metabolism (2014) **34,** 1599–1603; doi:10.1038/jcbfm.2014.144; published online 6 August 2014

Keywords: astrocytes; BOLD; calcium; fMRI; IP_3; local field potentials

INTRODUCTION

Blood oxygenated level-dependent functional magnetic resonance imaging (BOLD fMRI) is an imaging technique used to monitor neuronal activity noninvasively, being currently a fundamental tool in basic and clinical investigations of the central nervous system. As many other neuroimaging methods, it relies on the fact that brain can adapt its blood flow to counterbalance the neuronal needs of oxygen and nutrients. The relationship between local neural activity and subsequent changes in cerebral blood flow (CBF) is known as functional hyperemia (or neurovascular coupling). Functional MRI signals are highly correlated with the electrophysiologic local field potentials (LFPs), an aggregate measure of synaptic and active dendritic currents.[1,2] Nevertheless, the exact mechanism that accounts for this neurovascular coupling remains unclear.[3]

Evidence suggest that astrocytes have an important role in linking neurotransmitter activity to vascular responses[4,5] and thus calcium-dependent release of vasoactive gliotransmitters has been widely suggested to trigger vasodilation. G protein-mediated calcium signaling in astrocytes is mainly dependent on inositol trisphosphate receptor type 2 (IP_3R2).[6] Its activation allows calcium releases from intracellular stores[7] and is critical for astrocytic Ca^{2+} surges in the hippocampus[8] and the cortex.[9] Of potential interest for the interpretation of functional neuroimaging data is the fact that Ca^{2+} transients in astrocytes can be induced by nonneuronal activity and are not necessarily independent of ongoing metabolic processes in this cell type.[10] Therefore, a contribution of astrocytes to CBF regulation unrelated to neuronal activity cannot be discarded and, as a consequence, the interpretation of BOLD fMRI signals could be biased.

In the current study, we investigated the quantitative relevance of IP_3-dependent calcium signaling in astrocytes for the generation of fMRI signals. For that purpose, we recorded LFP and BOLD signals in the hippocampus of IP_3R2 knockout (KO) mice during different protocols of monosynaptic electrical stimulation.

MATERIALS AND METHODS

Animals

All animal procedures were approved by the corresponding ethical committee (IN-CSIC) and were performed in accordance with Spanish (law 32/2007) and European regulations (EU directive 86/609, EU decree 2001-486) and with the ARRIVE guidelines.

Four-month C57Bl6/J male mice were housed in cages of four animals, with a 12-hour diurnal light cycle with food and water *ad libitum*. The IP_3R2 KO mice were generously donated by Dr J Chen.[11]

Electrophysiology

Mice (~35 g) were anesthetized with 1% to 1.5% isoflurane in oxygen at 0.4 L per minute. Temperature, oxygen saturation, heart, and breathing rates were continuously monitored (MouseOx, PanLab—Harvard Apparatus, Barcelone, Spain). Bupivacaine (0.5%, B.Braun) was injected subcutaneously under the scalp 15 minutes before the surgery. Two craniotomies were performed over the hippocampus (from bregma: − 2 mm antero-posterior, 1.2 mm medio-lateral) and perforant pathway (from lambda: antero-posterior 0 mm, medio-lateral 2.6 mm) to implant recording and stimulating electrodes, respectively. Local field potentials were recorded using a 32 channel electrode (NeuroNexus, Ann Arbor, MI, USA) located across the CA1 and dentate gyrus (DG) fields of the hippocampus. Stimulating electrodes were made of platinum-iridium wire (A-M Systems, Sequim, WA, USA) as before. Excitatory postsynaptic potentials (EPSPs) were recorded in the molecular layer of the DG and population spikes (PSs) in the hilus of the DG.

Stimulation Protocols

The entorhinal cortex input to the hippocampus was stimulated using three different protocols. Single pulse stimulus to build intensity/response

[1]Centre of Excellence Severo Ochoa, Consejo Superior de Investigaciones Científicas, Universidad Miguel Hernández, Sant Joan d'Alacant, Spain; [2]Instituto Cajal, CSIC, Madrid, Spain and [3]Department of Neuroscience, University of Minnesota, Minneapolis, Minnesota, USA. Correspondence: Dr S Canals, Centre of Excellence Severo Ochoa, CSIC-UMH, Campus de San Juan, Avenida Ramón y Cajal, s/n, Sant Joan d'Alacant 03550, Spain.
E-mail: scanals@umh.es

The authors are grateful to Begoña Fernández for excellent technical assistance. Research at SC laboratory is supported by grants from the Spanish MINECO (BFU2012-39958 and PIM2010ERN-00679 as part of the Era-Net NEURON TRANSALC project). PJ has been supported by the 'Symbad' Marie Curie ITN program.
Received 4 June 2014; revised 17 July 2014; accepted 18 July 2014; published online 6 August 2014

curves was delivered to the perforant pathway from 50 to 1,200 μA, at a frequency of 0.05 Hz (5 repetitions per intensity in total). Trains of pulses at 10 Hz were also delivered to the perforant pathway with stimulus intensities producing half maximal PS in the hilus (300 to 500 μA). Two train durations, 4 and 20 seconds, were used in both electrophysiologic and fMRI experiments. Each train was repeated in a block design with resting periods of 60 seconds between stimulation epochs. Stimulation pulses were always biphasic and charge balanced, with the cathodal pulse leading and a pulse duration of 0.2 ms. Electrical stimulation was delivered using a current source and pulse generator STG 2004 (Multichannel Systems, Reutlingen, Germany).

Functional Magnetic Resonance Imaging Study

After electrophysiologic recordings were completed, the multichannel recording electrode was removed and the stimulating electrode secured to the skull with dental cement. Animals were fixed in an MRI compatible cradle with ear and bite bars. Functional MRI data were acquired under dexmedetomidine anesthesia since it has been reported to preserve reliable and high amplitude BOLD responses compared with isoflurane.[12] After an initial bolus of 0.4 mg/kg subcutaneously, isoflurane was progressively discontinued and substituted by a continuous infusion of dexmedetomidine (subcutaneously 0.8 mg/kg per hour).[12] In our hands, the above regime of dexmedetomidine induces a stable anesthetic plane with constant physiologic parameters (oxygen saturation, pulse distension, breathing, and heart rate) during no more than 2 hours. Since the completion of the electrophysiologic recordings together with fMRI measurements requires longer times, we performed the electrophysiology under isoflurane and then switch to dexmedetomidine for fMRI. In a set of preliminary experiments, we first recorded and compared the evoked electrophysiologic potentials in the DG under both anesthetic regimes (data not shown). No statistically significant differences between both anesthetics were found in the electrophysiologic response (PS amplitude) to a 10- Hz, 4 -secondslong stimulation train (40 pulses) as the ones used for fMRI (two-way analysis of variance for anesthesia and pulse number in the train, $P > 0.05$ for both factors, $n = 3$).

Functional MRI experiments were performed in a horizontal 7-Tesla scanner with a 30-cm diameter bore (Biospec 70/30v, Bruker Medical, Ettlingen, Germany). Functional MRI was done in 12 coronal slices using a Gradient Echo Echo-Planar Imaging sequence with the following parameters: field of view 20×20 mm, slice thickness 1 mm, matrix 96×96, segments 1, flip angle 60°, echo time 15 ms, and repetition time 2,000 ms. As anatomic reference for the functional maps, T_2-weighted anatomic images were collected using a rapid acquisition relaxation enhanced sequence: field of view 20×20 mm, 12 slices, slice thickness 1 mm, matrix 192×192, effective echo time 56 ms, repetition time 2,000 ms, and a rapid acquisition relaxation enhanced sequence factor of 8.

Data Analysis

The EPSPs were quantified as the maximal slope of the negative-going potential recorded in the molecular layer and the PS as the amplitude between the negative peak and its preceding positivity of the potential recorded in the center of the hilus. Functional MRI data were analyzed offline using custom-made software developed in MATLAB and with the statistical parametric mapping packages (SPM8, www.fil.ion.ucl.ac.uk/spm). Functional maps were generated from voxels that have a significant component for the model and are clustered together in space ($P < 0.01$ corrected). The propagation of functional activity was computed as the number of statistically significant voxels in a region of interest containing the hippocampal formation. The intensity of activation was computed as the average BOLD signal increase in the hippocampal region of interest (no statistical threshold applied) during stimulation and expressed as percentage of the prestimulation epochs.

RESULTS AND DISCUSSION

In the present study, we compare the electrophysiologic signature and fMRI responses in the hippocampus to direct electrical stimulation of the perforant pathway in IP_3R2 KO mice and their background strain C57BL7/6J mice (wild type, WT).

Single pulses at different intensities delivered to the perforant pathway produced the characteristic field potentials in the molecular layer (EPSP) and hilus (PS) of the DG. The waveforms, slope of the EPSP and PS amplitude and thus the input/output curves were undistinguishable in both WT and KO mice (Figures 1A to 1D). The latencies of the EPSP and PS were also identical in both genotypes (Figures 1A and 1B, insets). These results indicate that loss of IP_3R2-dependent calcium signaling in hippocampal astrocytes does not affect neuronal excitability or evoked synaptic activity of DG granule cells to perforant pathway stimulation, in good agreement with previous results for CA1 pyramidal neurons.[8] Since alterations in cholinergic-induced synaptic plasticity have been reported in IP_3R2 KO animals,[9,13,14] the results also suggest that neuronal modulation and synaptic plasticity may rely on diverse neuronal and astrocytic mechanisms (a recent review and discussion of this issue can be found in Araque *et al*[15]). Next, we tested whether the response to trains of stimuli, as those required for eliciting robust fMRI signals,[16] was altered. The averaged EPSP slope and PS amplitude evoked by short (4 seconds, Figure 1E) as well as long (20 seconds, Figure 1F) trains of stimuli delivered to the perforant pathway were not statistically different in WT and KO mice. The dynamic evolution of evoked potentials inside the trains was also comparable in both genotypes (Supplementary Figures 1 and 2), with a tendency toward smaller activations in the last pulses of the long stimulus protocol in the KO animals (Supplementary Figure 1B).

Having recorded comparable baseline electrophysiologic response in IP_3R2 KO and WT mice, we then tested in the same animals the short- and long-lasting stimulation protocols for eliciting BOLD signals in the hippocampus. Neither the extension of the activity maps across ipsilateral and contralateral hippocampal subfields (Figures 2A and 2B) nor the amplitude of the signals (Figures 2B and 2C) or the kinetics of the BOLD response (Figures 2C and 2D) were significantly altered in the absence of IP_3R2-dependent Ca^{2+} surges in astrocytes. It has been proposed that astrocytes may contribute primarily to the maintenance of hemodynamic response rather than its initiation.[17] Our results comparing 4- and 20-second stimulation protocols (Figures 2E and 2F) show that the kinetic of the BOLD signals are virtually identical at the initiation phase and maintenance, in WT and IP_3R2 KO mice. Overall, these results discard an IP_3R2-mediated contribution of astrocytes to the fMRI signal generation or the evoked neurotransmission.

Our findings complement and extend recent reports showing intact vasodilatory responses in IP_3R2 KO mice. Devor and colleagues using brief stimulations (2 seconds) of the forelimb and two-photon imaging showed in WT animals that Ca^{2+} signals in astrocytes in the sensory cortex lag behind the vascular responses and these ones are indistinguishable from those in the KO animals.[18] The result was consistent with a previous report showing that blocking mGluR type 5 upstream of the IP_3-dependent calcium release from intracellular stores did not affect the hemodynamic response in the barrel cortex to a brief sensory stimulus.[19] In a different study[20] the authors used laser doppler flowmetry and direct stimulation of the largely cholinergic nucleus basalis of Meynert to increase CBF and show intact hemodynamic responses in the cortex of IP_3R2 KO animals. The authors also show intact CBF responses in barrel cortex to 20 seconds stimulation of the vibrissa. Our results build on these findings to show that the amplitude and kinetic of the BOLD fMRI signals upon stimulation of the perforant pathway are not altered in IP_3R2 KO mice, in the presence of normal neurotransmission. This result holds true for both, short and long stimulation epochs discarding a role of IP_3R2 in the maintenance, as well as the initiation, of the functional response. Furthermore, by using fMRI we show that the extension of the activity map in the brain is also preserved, discarding a role of IP_3R2-dependent calcium waves in propagating functional hyperemic responses through the astrocytes syncytium.

Collectively, these results challenge the view of IP_3-mediated Ca^{2+} changes in astrocytes as the link between the increase in local neuronal activity and vascular responses. Compensatory

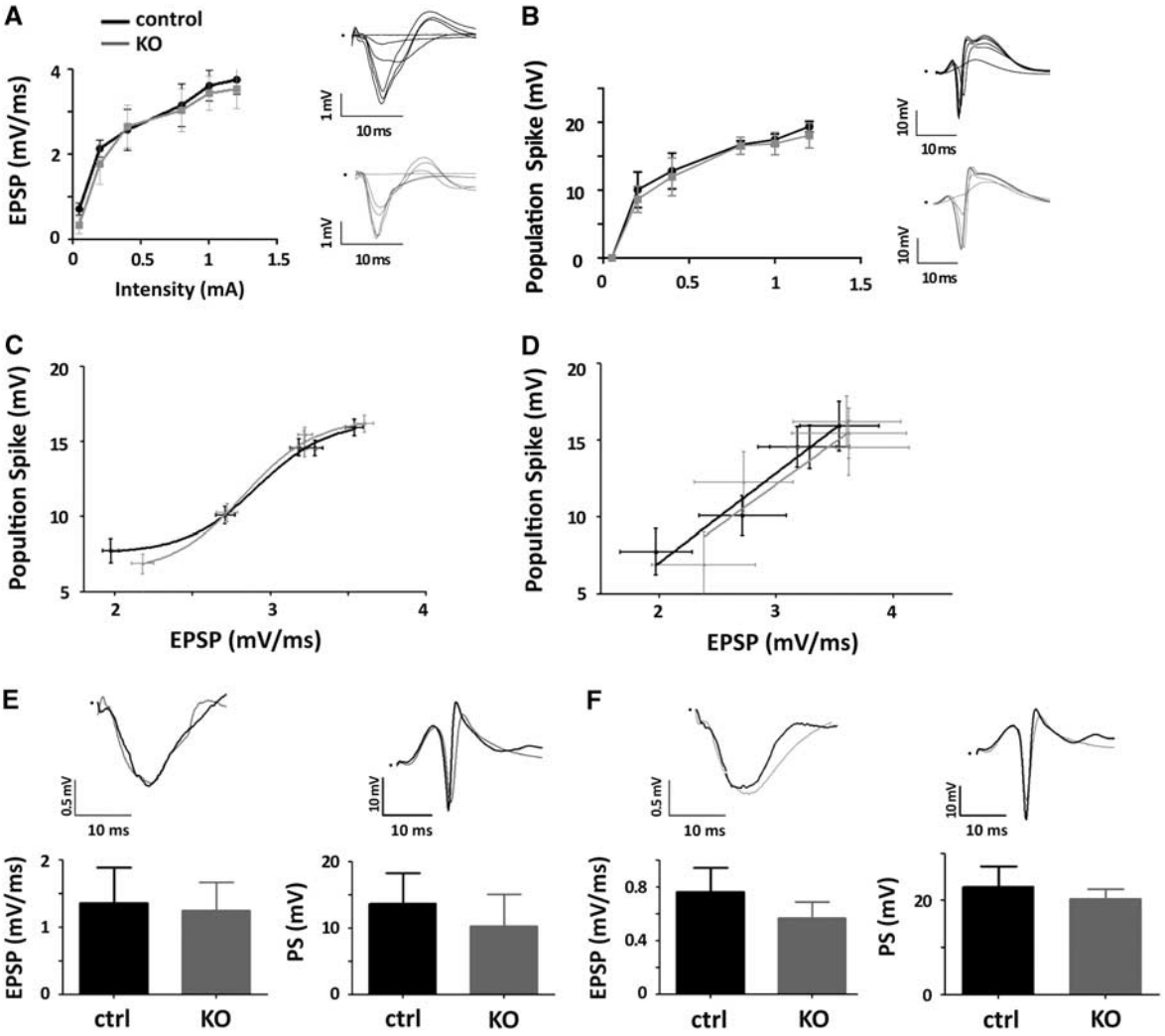

Figure 1. Electrophysiologic responses in the dentate gyrus (DG) of inositol trisphosphate receptor type 2 (IP_3R2) knockout (KO) mice to perforant path stimulation. (**A**) Excitatory postsynaptic potential (EPSP) slope in response to single pulse stimulation delivered to the perforant pathway (PP) at increasing intensities from 0.05 to 1.2 mA. Insets show representative evoked potentials recorded in the molecular layer for different stimulation intensities. Black tracings are used for wild-type control animals and gray tracings for IP_3R2 KO mice. (**B**) Same as (**A**) but for the population spike (PS) recorded in the center of the hilus of the DG. (**C**) Input/output curves (EPSP/PS) of one control and one KO animal over the whole range of stimulations. (**D**) Input/Output curves for the linear range of stimulations averaged across the population of control ($n = 18$) and KO animals ($n = 11$). Data are fitted using linear regression with slopes and elevations showing no statistically significant differences ($P = 0.879$ and 0.449, respectively). (**E**) Average local field potentials (LFPs) recorded during a brief 4-second train stimulation of the PP at 10 Hz. No statistically significant differences (two-tail *T*-test) were found neither for the EPSP ($P = 0.58$) nor for the PS ($P = 0.10$) between control and KO animals ($n = 18$ and $n = 11$, respectively). (**F**) Average of LFPs recorded during the long 20-second train stimulation of the PP at 10 Hz. No statistically significant differences (two-tail *T*-test) were found neither for the EPSP ($P = 0.16$) nor for the PS ($P = 0.37$) between control and KO animals ($n = 5$ and $n = 3$, respectively).

effects after a constitutive genetic deletion, as in the IP_3R2 KO animal, cannot be fully discarded. However, previous experiments using these animals have importantly showed a loss of Ca^{2+} activity in astrocytic cell bodies and perivascular endfeet (both spontaneous activity and evoked by neuronal stimulation or pharmacological manipulations of G_q-linked G-protein-coupled receptors) without any apparent compensation, and in the presence of an intact Ca^{2+} activity in neurons.[9,13,14] Different cell types and physiologic and metabolic compartments have been proposed to contribute to the generation of functional hemodynamic responses.[2] Our results, however, do not discard the potential contribution of astrocytes to CBF regulation through different molecular mechanisms not requiring IP_3R2-mediated Ca^{2+} surges. For instance, pericytes have recently been shown to be largely involved in vasodilation[21] and their activation could be in part mediated through astrocytes. While further investigation is required to elucidate the mechanisms supporting neurovascular coupling, an important consideration is the potential contribution of cell types and signaling pathways independently of neuronal activation. It has been hypothesized that astroglial function unrelated to neuronal activity could be reflected in fMRI measurements.[10] The evidence discussed here indicates that the modulation of Ca^{2+} signals in astrocytes is not likely contributing to functional brain imaging.

DISCLOSURE/CONFLICT OF INTEREST

The authors declare no conflict of interest.

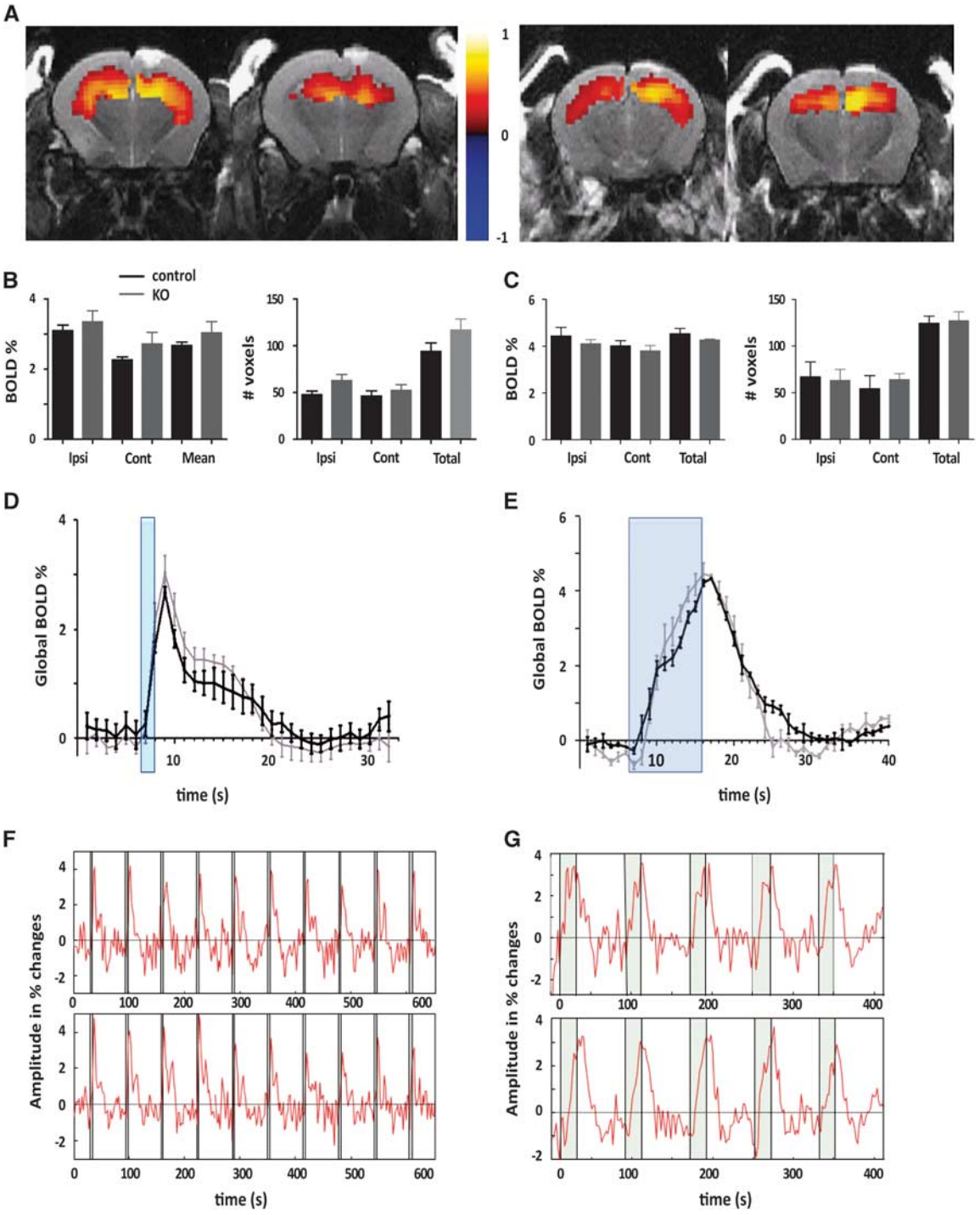

Figure 2. Initiation and maintenance of blood oxygenated level-dependent functional magnetic resonance imaging (BOLD fMRI) signals in the hippocampus of inositol trisphosphate receptor type 2 (IP_3R2) knockout (KO) mice. (**A**) Representative example of BOLD fMRI maps in the hippocampus of wild-type control (*left*) and KO (*right*) mice upon stimulation of the perforant pathway (PP) at 10 Hz. Functional maps are color coded and overlaid on T2-anatomic scans. The color code represents the correlation (*R* value) of the BOLD signal with the stimulation paradigm. (**B**) *Left,* BOLD activation during the brief 4-second stimulation in the ipsilateral (ipsi) and contralateral hippocampus (contra) and over the whole brain (two-tail *t*-test; $P=0.44$, $P=0.14$, and $P=0.23$, respectively) (wild type, WT $n=11$; KO $n=9$); *Right*, Number of voxels activated during the brief 4-second stimulation in the ipsilateral hippocampus (ipsi HP), contralateral HP (contra) and in total ($P=0.051$, $P=0.49$, and $P=0.15$ respectively). (**C**) Global BOLD signal kinetics during 4-second stimulation, the stimulation period is marked in blue. It represents the average of 3 repetitions of 10 stimulations per animal (WT $n=11$; KO $n=9$). (**D**) Representative example of a BOLD time course during a short stimulation in WT (upper panel) and KO (lower panel). (**E**–**G**) Same as (**B**–**D**) but for the long 20-second stimulation protocol. No statistically significant differences were found for any of the measured parameters (two-tail *t*-test, WT $n=3$, KO $n=3$).

REFERENCES

1 Logothetis NK. What we can do and what we cannot do with fMRI. *Nature* 2008; **453**: 869–878.
2 Moreno A, Jego P, de la Cruz F, Canals S. Neurophysiological, metabolic and cellular compartments that drive neurovascular coupling and neuroimaging signals. *Front Neuroenergetics* 2013; **5**:3.
3 Lauritzen M, Mathiesen C, Schaefer K, Thomsen KJ. Neuronal inhibition and excitation, and the dichotomic control of brain hemodynamic and oxygen responses. *NeuroImage* 2012; **62**: 1040–1050.
4 Zonta M, Angulo MC, Gobbo S, Rosengarten B, Hossmann KA, Pozzan T *et al.* Neuron-to-astrocyte signaling is central to the dynamic control of brain microcirculation. *Nat Neurosci* 2003; **6**: 43–50.
5 Attwell D, Buchan AM, Charpak S, Lauritzen M, Macvicar BA, Newman EA. Glial and neuronal control of brain blood flow. *Nature* 2010; **468**: 232–243.
6 Holtzclaw LA, Pandhit S, Bare DJ, Mignery GA, Russell JT. Astrocytes in adult rat brain express type 2 inositol 1,4,5-trisphosphate receptors. *Glia* 2002; **39**: 69–84.
7 Parpura V, Haydon PG. Physiological astrocytic calcium levels stimulate glutamate release to modulate adjacent neurons. *Proc Natl Acad Sci USA* 2000; **97**: 8629–8634.
8 Petravicz J, Fiacco TA, McCarthy KD. Loss of IP3 receptor-dependent Ca^{2+} increases in hippocampal astrocytes does not affect baseline CA1 pyramidal neuron synaptic activity. *J Neurosci* 2008; **28**: 4967–4973.
9 Takata N, Mishima T, Hisatsune C, Nagai T, Ebisui E, Mikoshiba K *et al.* Astrocyte calcium signaling transforms cholinergic modulation to cortical plasticity in vivo. *J Neurosci* 2011; **31**: 18155–18165.
10 Wang X, Takano T, Nedergaard M. Astrocytic calcium signaling: mechanism and implications for functional brain imaging. *Methods Mol Biol (Clifton, N.J.)* 2009); **489**: 93–109.
11 Li X, Zima AV, Sheikh F, Blatter LA, Chen J. Endothelin-1-induced arrhythmogenic Ca^{2+} signaling is abolished in atrial myocytes of inositol-1,4,5-trisphosphate(IP3)-receptor type 2-deficient mice. *Circ Res* 2005; **96**: 1274–1281.
12 Adamczak JM, Farr TD, Seehafer JU, Kalthoff D, Hoehn M. High field BOLD response to forepaw stimulation in the mouse. *NeuroImage* 2010; **51**: 704–712.
13 Navarrete M, Perea G, Fernandez de Sevilla D, Gomez-Gonzalo M, Nunez A, Martin ED *et al.* Astrocytes mediate in vivo cholinergic-induced synaptic plasticity. *PLoS Biol* 2012; **10**: e1001259.
14 Di Castro MA, Chuquet J, Liaudet N, Bhaukaurally K, Santello M, Bouvier D *et al.* Local Ca^{2+} detection and modulation of synaptic release by astrocytes. *Nat Neurosci* 2011; **14**: 1276–1284.
15 Araque A, Carmignoto G, Haydon PG, Oliet SH, Robitaille R, Volterra A. Gliotransmitters travel in time and space. *Neuron* 2014; **81**: 728–739.
16 Canals S, Beyerlein M, Murayama Y, Logothetis NK.. Electric stimulation fMRI of the perforant pathway to the rat hippocampus. *Magn Reson Imaging* 2008; **26**: 978–986.
17 Koehler RC, Roman RJ, Harder DR.. Astrocytes and the regulation of cerebral blood flow. *Trends Neurosci* 2009; **32**: 160–169.
18 Nizar K, Uhlirova H, Tian P, Saisan PA, Cheng Q, Reznichenko L *et al.* In vivo stimulus-induced vasodilation occurs without IP3 receptor activation and may precede astrocytic calcium increase. *J Neurosci* 2013; **33**: 8411–8422.
19 Calcinaghi N, Jolivet R, Wyss MT, Ametamey SM, Gasparini F, Buck A *et al.* Metabotropic glutamate receptor mGluR5 is not involved in the early hemodynamic response. *J Cereb Blood Flow Metab* 2011; **31**: e1–10.
20 Takata N, Nagai T, Ozawa K, Oe Y, Mikoshiba K, Hirase H. Cerebral blood flow modulation by basal forebrain or whisker stimulation can occur independently of large cytosolic Ca^{2+} signaling in astrocytes. *PLoS ONE* 2013; **8**: e66525.
21 Hall CN, Reynell C, Gesslein B, Hamilton NB, Mishra A, Sutherland BA *et al.* Capillary pericytes regulate cerebral blood flow in health and disease. *Nature* 2014; **508**: 55–60.

Supplementary Information accompanies the paper on the Journal of Cerebral Blood Flow & Metabolism website (http://www.nature.com/jcbfm)